AMERICAN SOCIETY FOR MICROBIOLOGY | mSphere

Check for updates

| Parasitology | Research Article

Targets for the diagnosis of *Acanthamoeba* eye infections include four cyst wall proteins and the mannose-binding domain of the trophozoite mannose-binding protein

Bharath Kanakapura Sundararaj,[1] Manish Goyal,[1] John Samuelson[1]

AUTHOR AFFILIATION See affiliation list on p. 17.

ABSTRACT *Acanthamoebae*, which are free-living amoebae, cause corneal inflammation (keratitis) and blindness, if not quickly diagnosed and effectively treated. The walls of *Acanthamoeba* cysts contain cellulose and have two layers connected by conical ostioles. Cysts are identified by *in vivo* confocal microscopy of the eye or calcofluor-white- or Giemsa-labeling of corneal scrapings, both of which demand great expertise. Trophozoites, which use a mannose-binding protein to adhere to keratinocytes, are identified in eye cultures that delay diagnosis and treatment. We recently used structural and experimental methods to characterize cellulose-binding domains of Luke and Leo lectins, which are abundant in the inner layer and ostioles. However, no antibodies have been made to these lectins or to a Jonah lectin and a laccase, which are abundant in the outer layer. Here, confocal microscopy of rabbit antibodies (rAbs) to recombinant Luke, Leo, Jonah, and laccase supported localizations of GFP-tagged proteins in walls of transfected *Acanthamoebae*. rAbs efficiently detected calcofluor white-labeled cysts of 10 of the 11 *Acanthamoeba* isolates tested, including six T4 genotypes that cause most cases of keratitis. Further, laccase shed into the medium during encystation was detected by an enzyme-linked immunoassay. Structural and experimental methods identified the mannose-binding domain (ManBD) of the *Acanthamoeba* mannose-binding protein, while rAbs to the ManBD efficiently detected DAPI-labeled trophozoites from all 11 *Acanthamoeba* isolates tested. We conclude that antibodies to four cyst wall proteins and the ManBD efficiently identify *Acanthamoeba* cysts and trophozoites, respectively.

IMPORTANCE Free-living amoeba in the soil or water cause *Acanthamoeba* keratitis, which is diagnosed by identification of unlabeled cysts by *in vivo* confocal microscopy of the eye or calcofluor-white (CFW) labeled cysts by fluorescence microscopy of corneal scrapings. Alternatively, *Acanthamoeba* infections are diagnosed by the identification of trophozoites in eye cultures. Here, we showed that rabbit antibodies (rAbs) to four abundant cyst wall proteins (Jonah, Luke, Leo, and laccase) each efficiently identify CFW-labeled cysts of 10 of the 11 *Acanthamoeba* isolates tested. Further, laccase released into the medium by encysting *Acanthamoebae* was detected by an enzyme-linked immunoassay. We also showed that rAbs to the mannose-binding domain (ManBD) of the *Acanthamoeba* mannose-binding protein, which mediates adherence of trophozoites to keratinocytes, efficiently identify DAPI-labeled trophozoites of all 11 *Acanthamoeba* isolates tested. In summary, four wall proteins and the ManBD appear to be excellent targets for the diagnosis of *Acanthamoeba* cysts and trophozoites, respectively.

KEYWORDS *Acanthamoeba*, AlphaFold, cyst, cyst wall proteins, diagnosis, ELISA, keratitis, lateral gene transfer, mannose-binding protein, rabbit antibodies, trophozoite

Editor Katherine S. Ralston, University of California, Davis, Davis, California, USA

Address correspondence to John Samuelson, jsamuels@bu.edu.

Bharath Kanakapura Sundararaj and Manish Goyal contributed equally to this article. Bharath Kanakapura Sundararaj is listed first because he inititated the experiments.

The authors declare no conflict of interest.

See the funding table on p. 18.

Received 5 November 2024
Accepted 31 January 2025
Published 4 March 2025

Acanthamoeba is an important eye pathogen in the under-resourced countries, where agricultural work increases the risk of scratches to eyes and water for handwashing is scarce (1–4). *Acanthamoeba* is an emerging pathogen in the United States and Europe, where contact lens use is frequent while swimming in fresh water that contains free-living amoebae (5–7). Regardless of the geographic location or route of infection, 18S RNA sequences show T4 genotypes, which include the genome project Neff strain of *Acanthamoeba castellanii* (Ac), most often cause corneal inflammation (keratitis) (8–15).

Acanthamoebae cause keratitis when trophozoites adhere to corneal cells via a mannose-binding protein (called here AcMBP) to distinguish it from host mannose-binding proteins (16). Monoclonal antibodies have been made to AcMBP, which may be used to identify trophozoites in cultures of corneal smears, while a domain of unknown function (DUF4114) has been suggested as the mannose-binding domain (ManBD) of *Acanthamoeba castellanii* mannose-binding protein (AcMBP-1) but has not been experimentally proven (17–22). Adherent trophozoites release proteases and pore-forming peptides, which cause corneal ulcers, scars, and blindness, if not successfully diagnosed and treated (23–30).

Acanthamoeba cysts, which form when trophozoites are starved of nutrients, have a cellulose- and chitin-rich wall with two layers (ectocyst and endocyst) connected by conical ostioles (31–37). Cyst walls protect free-living *Acanthamoebae* in fresh water, which lyses trophozoites. Further, cyst walls protect *Acanthamoebae* from killing by disinfectants used to clean surfaces, sterilizing agents in contact lens solutions, and alcohols in hand sanitizers (38–43).

In resourced countries, *Acanthamoeba* keratitis (AK) may be diagnosed by identification of unlabeled cysts by *in vivo* confocal microscopy of the cornea, although the instrument and expertise are both rare (44–49). Alternatively, AK is diagnosed by the identification of cysts labeled with calcofluor-white (CFW) or Giemsa in corneal scrapings. Regardless of the method, great skill is needed as *Acanthamoeba* cysts may easily be confused with either plant cells or fungi, which irritate the cornea or cause keratitis, respectively (38, 50–53). AK can also be diagnosed by identification of trophozoites in cultures of corneal smears, which are typically inefficient and delay treatment for weeks. In contrast, *Giardia lamblia* and *Cryptosporidium parvum* and *hominem*, which cause severe diarrhea, are diagnosed by monoclonal antibodies to cyst and oocyst wall proteins, respectively, in human stool samples, while monoclonal antibodies to the Jacob lectin in cyst walls distinguish *Entamoeba histolytica*, which causes dysentery and liver abscess, from the more benign *E. dispar* (54–56).

The primary goal of the present studies is to test whether abundant proteins in the ectocyst layer (Jonah and laccase) or endocyst layer and ostioles (Luke and Leo), which we identified by mass spectrometry of purified walls and localized by GFP-tagging, are good targets for diagnostic anti-cyst rabbit antibodies (rAbs) (33, 35, 57, 58). Jonah lectins contain one or three β-helical folds (BHFs) like those of Antarctic bacteria, while Ac laccases have three copper oxidase (CuRO) domains like those of bacterial spore coat proteins (59–61). Luke lectins contain two or three β-jelly-roll folds (BJRFs) like those of cellulose-binding domains of bacterial and plant endocellulases, while sets of four disulfide knots (4DKs) of Leo are unique to *Acanthamoeba* (62–66).

Here, we determine the efficiency of rAbs to Jonah-1, laccase-1, Luke-2, and Leo-A to detect CFW-labeled cysts of 11 isolates of *Acanthamoeba*, including seven T4 genotypes that cause most cases of AK in resourced and under-resourced countries (8, 9, 11, 12, 14, 67). We also test the ability of rAbs to the ManBD of AcMBP, which we proved by its ability to bind to a mannose-agarose resin and to human corneal limbal epithelial (HCLE) cells, to detect DAPI-labeled trophozoites of the same 11 isolates of *Acanthamoeba* (18–21, 68).

RESULTS

With a single caveat, sequence searches with BLASTP and TBLASTN strongly support the four wall proteins chosen for making rAbs for the diagnosis of *Acanthamoeba* cysts in corneal scrapings

Rabbits were immunized with an *Escherichia coli* maltose-binding protein (EcMBP)-fused to the BHF of Jonah-1 (ACA1_164810), two BJRFs of Luke-2 (ACA1_377670), two sets of 4DKs of Leo-A (ACA1_074730), and the first copper oxidase (CuRO-1) domain of an abundant laccase-1 (ACA1_068450), the AlphaFold structures of which are shown in Fig. 1A, B, G and H (8, 9, 33, 63, 69, 70). See Fig. S1 for their amino acid sequences and that of the ManBD of AcMBP-1, which is described below. Sequence alignments with BLASTP, which did not include the low complexity spacers that are poorly conserved, showed that the N-terminal BJRF of recombinant Luke-2 was duplicated in Neff strain (ACA1_377510), while the N- and C-terminal 4DKs of recombinant Leo-A have a close paralog (ACA1_083920) (59, 71, 72). The other 15 Luke lectins and 13 Leo lectins, as well as the BHFs of seven other Jonah lectins, of the Neff strain of Ac show <60% positional identities, so that rAbs to recombinant Luke, Leo, and Jonah are unlikely to cross-react with paralogous wall proteins. In contrast, TBLASTN searches of 18 other *Acanthamoeba* genomes in AmoebaDB, the proteins of which have not been predicted, showed the vast majority have >85% positional identity with recombinant Luke, Leo, and Jonah and so are very likely to be detected by rAbs to each protein (8, 9, 73).

The caveat here is the CuRO-1 domain of Ac laccase-1, which has sequences (TMWYHDH and NVYAGLAGFYLLRD) conserved in two other Ac laccases (ACA1_006180 and ACA1_008840) and partially conserved in laccases of bacteria (e.g., *Clostridium* and *Bacillus*), fungi (*Bifiguratus*), and plants (*Daucus*) (Fig. S2) (59, 71, 72). These results, which suggest the possibility that anti-laccase-1 rAbs might cross-react with bacteria, fungi, or plant cells in the eye, are not surprising, because laccase is a well-conserved enzyme (74). TBLASTN showed that all *Acanthamoeba* genomes in AmoebaDB have >90% positional identities with Curo-1 of Neff strain and so are likely to efficiently bind anti-laccase-1 rAbs.

Confocal microscopy of rAbs binding to intact cysts and broken walls of the Ac Neff strain generally confirms the localization of tagged wall proteins

The goal here was to determine whether rAbs to four wall proteins localize to the same place in cyst walls of the Neff strain of Ac (confirmed by the sequence of its 18S RNA) as do tagged proteins expressed under their own promoters (33, 35). We used confocal microscopy to compare the binding of pairs of rAbs to broken and intact walls of non-transfected Neff strain cysts (with the localization of pairs of tagged proteins, each expressed under its own promoter, in walls of transfected Ac (Fig. 1C and I). Double labels showed Jonah-1-mCherry has a patchy distribution in the ectocyst layer of intact and broken cyst walls of Ac, while Luke-2-GFP is more abundant in ostioles than the endocyst layer, which was labeled with CFW (Fig. 1D). Similarly, rAbs to the BHF of Jonah-1 labeled red the ectocyst layer of intact and broken cyst walls, while rAbs to two BJRFs of Luke-2 labeled green the ostioles of intact cysts and the endocyst layer of broken cysts (Fig. 1E). In contrast, the negative control, which is pre-bleed rAbs, did not bind to intact or broken cysts (Fig. 1F).

Laccase-1-RFP had a patchy distribution in the ectocyst layer of intact and broken cyst walls of Ac, while Leo-A-GFP was more abundant in the endocyst layer than in the ostioles (Fig. 1J). The rAbs to Curo-1 domain of laccase-1 labeled the ectocyst layer of both intact cyst and broken walls, while rAbs to two 4DKs of Leo-A more heavily labeled the endocyst layer of intact cysts and the ostioles of broken walls (Fig. 1K). In summary, localizations of rAbs to wall proteins matched well localization of tagged proteins.

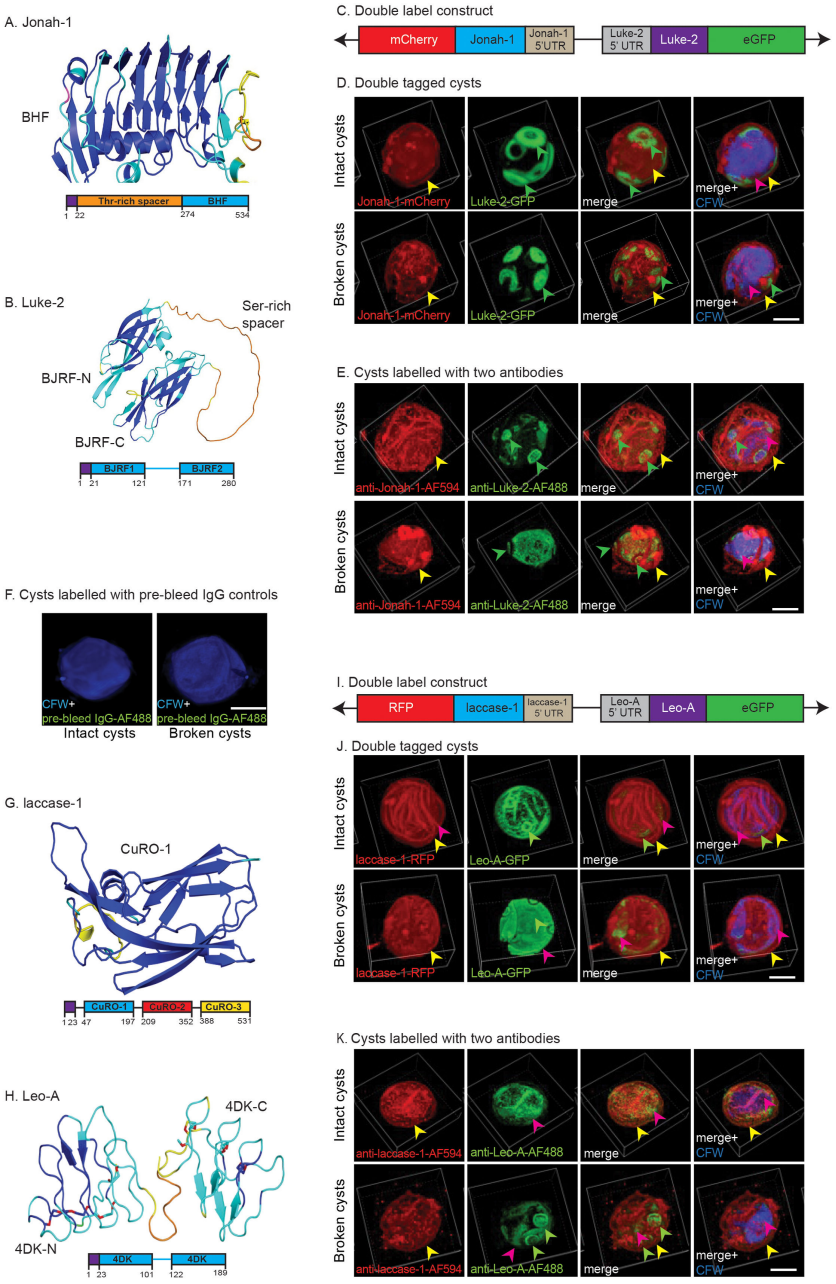

FIG 1 Double labels show rabbit antibodies (rAbs) to Jonah-1, Luke-2, laccase-1, and Leo-A localize to similar locations in intact cysts and broken cyst walls as do tagged proteins expressed under their own promoter in transfected *Acanthamoebae*. (A) AlphaFold with confidence colored shows the single BHF, which was used to make the EcMBP-Jonah-1 fusion-protein for production of anti-Jonah-1 rAbs. The diagram shows the N-terminal signal peptide (purple) and low complexity Thr-rich domain (orange). (B) AlphaFold shows N- and C-terminal BJRFs (BJRF-N and BJRF-C) connected by a low complexity spacer, which were used to make the EcMBP-Luke-2 fusion-protein to produce anti-Luke-2 rAbs. The diagram shows the N-terminal signal peptide (purple) and the low-complexity Ser-rich domain. (C) The first plasmid for double-labeling cyst walls contains full-length Jonah-1 cDNA with 574 bp of its 5′ UTR and a C-terminal mCherry tag head-to-head with full-length Luke-2 cDNA with 446 bp of its 5′ UTR and a C-terminal GFP tag (33). (D) Double labels show Jonah-1-mCherry is present in the ectocyst layer (yellow arrowheads) of intact and broken cysts, while Luke-GFP predominates in the ostioles (green arrowheads) of both preparations. CFW marks the endocyst layer (red arrowheads). (E) Anti-Jonah-1 rAbs

(Continued on next page)

Fig 1 (Continued)

(red) bind to the ectocyst layer of intact and broken cysts, while anti-Luke-2 rAbs (green) bind to ostioles of intact cysts and to the endocyst layer of broken walls. (F) Rabbit pre-bleeds fail to bind to intact cysts and broken walls. (G) AlphaFold shows the first copper oxidase domain (CuRO-1), which was used to make EcMBP-CuRO-1 for production of anti-laccase-1 rAbs. The diagram shows three CuRO domains in laccase-1. (H) AlphaFold shows N- and C-terminal sets of 4DKs (4DK-N and 4DK-C), which were used to make EcMBP-Leo-A for production of anti-Leo-A rAbs. The diagram shows the short spacer between sets of 4DKs of Leo-A. (I) The second plasmid for double-labeling cyst walls contains full-length laccase-1 cDNA with 405 bp of its 5′ UTR and a C-terminal RFP tag head-to-head with full-length Leo-A cDNA with 486 bp of its 5′ UTR and a C-terminal GFP. (J) Laccase-1-RFP is in the ectocyst layer of intact and broken cysts, while Leo-A-GFP is present in the endocyst layer and ostioles. (K) Anti-laccase-1 rAbs (red) bind to the ectocyst layer of intact and broken cysts, while anti-Leo-A rAbs (green) bind to the endocyst layer of intact cysts and to ostioles in broken walls. Scale bars for panels D–F, J, and K are 5 µm.

Despite numerous unexpected binding patterns, rAbs to Jonah-1, Luke-2, laccase-1, and Leo-A all efficiently detect CFW-labeled cysts of 10 of the 11 *Acanthamoeba* isolates

The goals here were to determine whether rAbs to cyst wall proteins bind to the same place in cyst walls of 10 other *Acanthamoeba* isolates as in the wall of the model Neff strain of Ac and to quantitatively measure how efficiently the rAbs detect CFW-labeled cysts. Eight *Acanthamoeba* isolates came from Dr. Monica Crary of Alcon Research, LLC, who studies their binding to contact lenses (39, 43). Two other *Acanthamoeba* isolates came from Dr. Noorjahan Panjwani, who identified AcMBP-1 on the surface of trophozoites (18–21). Segments of 18S RNA genes were amplified from trophozoites of each isolate, cloned, and sequenced to determine their similarity and genotype prior to encystation and testing with rAbs. A neighbor-joining tree of the 18S RNA sequences shows two pairs of isolates are identical (T4A-1/2 and T4B-1/2), while seven T4 isolates have short branch lengths and so closely resemble each other (Fig. S3). In contrast, genotypes T1, T11, T18, and T2/6C have long branch lengths and so are distinct from each other and from the T4 isolates.

Genotypes of *Acanthamoeba* were determined by matches to sequences compiled and treed by Paul Fuerst and others (Excel File 1) (8, 9, 11, 12, 14, 67). BLASTN searches determined the number of identical 18S RNA sequences at the NCBI, which was greatest for T4-Neff (36), T4A (25), T4B (17), and T4C (10) genotypes of *A. castellanii*. In contrast, identical 18S RNA sequences for T11 of *A. hatcheti* (5), T4D of *A. mauritaniensis* (4), T1 of *A. castellanii* (2), T2/T6C of *A. polyphaga* (1), and T18 of *A. byersi* (1) were rare. Finally, abundant isolates came from diverse sources (e.g., cornea, contact lenses, soil, and water for T4-Neff), while rare isolates came from brains (T1 and T18) of immunosuppressed patients with granulomatous amebic encephalitis (75).

High-power confocal microscopy showed rAbs to the BHF of Jonah-1 bound in a patchy distribution to the ectocyst layer of cysts of Neff strain and 10 other *Acanthamoeba* isolates (Fig. 1A and 2A). In contrast, rAbs to CuRO-1 domain of laccase-1 bound in a homogenous pattern to the Neff strain and to other *Acanthamoeba* isolates, which is like that of laccase-1-RFP (Fig. 1G, J and 2B). While rAbs to Luke-2 and Leo-A densely labeled the ostioles and weakly labeled the endocyst layer of cysts of the Neff strain and a few *Acanthamoeba* isolates (Fig. 1B, H, 2C and D), many other cysts were labeled on the ectocyst layer. There are two explanations, which are not mutually exclusive, for the variable distribution in the cyst walls of rAbs to Luke-2 and Leo-A. First, these proteins may be made at different times by different *Acanthamoeba* isolates, so that Luke-2 and Leo-A localize to different places (33). Second, these rAbs may bind to lesser amounts of Luke-2 and Leo-A in the ectocyst layer, which were not visualized by confocal microscopy, because of the large amounts of GFP-tagged Luke-2 and Leo-A in the endocyst layer and ostioles (Fig. 1D and J).

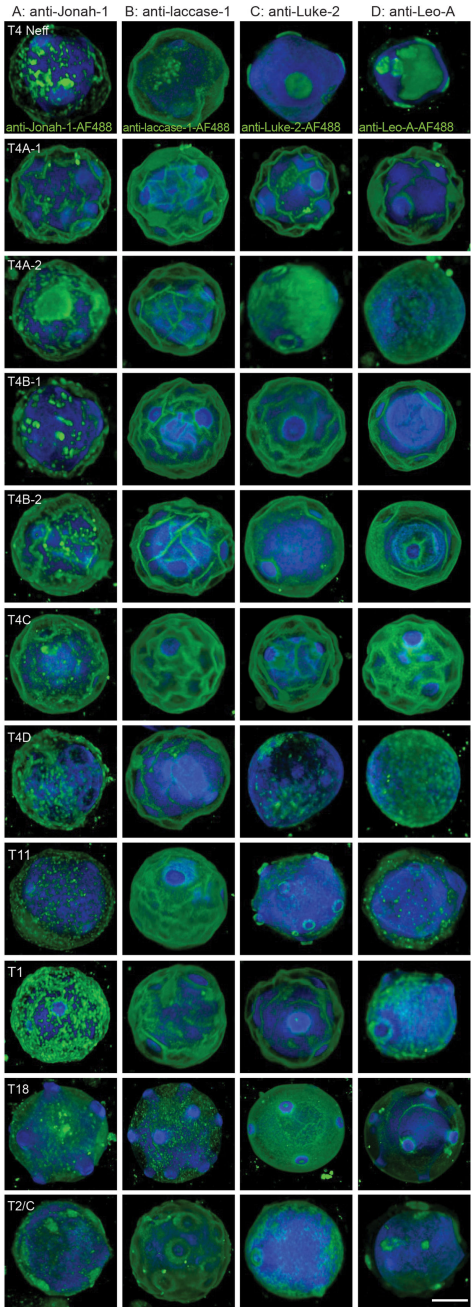

FIG 2 High-power confocal micrographs of 11 *Acanthamoeba* isolates show anti-Jonah-1 and anti-laccase-1 rAbs consistently bind to the surface of cysts, while anti-Luke-2 and anti-Leo-A rAbs bind to the endocyst layer and ostioles of some cysts (expected) and to the ectocyst layer of other cysts (unexpected). (A and B) The anti-Jonah-1 rAbs bind in a patchy distribution to the surface of cysts of 11 *Acanthamoeba* isolates, while the anti-laccase-1 rAbs bind in a homogenous manner. CFW labels the endocyst layer. (C and D) Both the anti-Luke-2 and anti-Leo-A rAbs bind to the ostioles and endocyst layer of some cysts of some genotypes (e.g., T4-Neff, T11, T18, and T2/6C) and the ectocyst layer of other cysts (e.g., T4A-1/2, T4B1/2, T4C, T4D, and T1) (see Fig. S3 and File S1 for characterization of genotypes). Possible reasons for the different patterns of binding of rAbs to Luke-2 and Leo-A are discussed in Results. A single scale bar for panels A–D is 5 µm. Random fields of rAbs binding to 11 *Acanthamoeba* isolates are shown in Fig. 3, while percentages of CFW-tagged cysts detected are shown in Fig. 4A.

To determine which wall proteins might be the best targets for diagnosis of cysts in AK, we counted in randomly selected fields the percentage of CFW-labeled cysts detected by rAbs to the four wall proteins (Fig. 3 and 4A). While the random fields are shown at low magnification in Fig. 3, rAb binding to CWF-labeled cysts was judged at magnifications like those shown in Fig. 2. Although there was variability in the intensity of binding of different rAbs to the same cyst genotype and of the same rAb to different genotypes, the rAbs to Luke-2, Leo-A, and laccase-1 each detected >95% of CFW-labeled cysts of 10 of the 11 *Acanthamoeba* isolates tested. In contrast, anti-Jonah-1 rAbs showed >95% detection for just 7 of the 11 *Acanthamoeba* isolates, suggesting that Jonah-1 might not be quite as good a target. In addition, all four rAbs struggled to detect cysts of genotype T4D (*A. mauritaniensis*), suggesting that there was a problem with encysting these trophozoites under the conditions used here. While counts were performed for two sets of cysts labeled with Protein-A Sepharose-purified antibodies, we observed similar results with rabbit sera diluted 1:300. Finally, we confirmed that rAbs to all four proteins were easily visible with a conventional fluorescence microscope, which is more likely to be present in a clinical setting than a confocal microscope (Fig. 4B).

Western blots show rAbs to recombinant Jonah-1, Luke-2, Leo-A, and laccase-1 bind to native wall proteins of the expected sizes and timing of expression, while enzyme-linked immunoassays (ELISAs) detect intact laccase-1 shed into the medium by encysting *Acanthamoebae*

In addition to confirming the size and timing of expression of each wall protein recognized by its rAbs, the goal here was to determine if any of the wall proteins are secreted into the culture medium during encystation and so might be detected using an ELISA (76). Western blots showed that pre-bleeds from rabbits do not react with proteins of trophozoites or cysts of the Neff strain of Ac (Fig. 4C). While rAbs to MBP-fusions with Jonah-1, Luke-2, Leo-A, and laccase-1 did not bind to trophozoite proteins, all rAbs bound well to cyst proteins. Anti-Jonah-1 rAbs bound to a protein of the expected size of ~55 kDa (red arrow), as well as to two lower molecular weight bands (blue arrows), which may result from proteolytic cleavage of Jonah-1. Anti-Luke-2 rAbs bound to a thick ~50 kDa band (red arrow), which is greater than the 27 kDa expected size of Luke-2. The increased size of Luke-2 is likely caused by extensive glycosylation of its five *N*-glycan sites and ~20 *O*-glycan sites in the low complexity, Ser-rich spacer (77–79). Anti-Leo-A rAbs bound to an ~13 kDa band (red arrow), which is slightly smaller than the expected size of 17 kDa, most likely due to the acidity of the protein that makes it run faster on SDS-PAGE. Anti-laccase-1 rAbs bound to a 75 kDa band (red arrow), which is slightly bigger than the expected size of 64 kDa and so likely caused by glycans, as well as to a less abundant 55 kDa band (blue arrow) caused by proteolytic cleavage.

Western blots of proteins of encysting Ac showed Jonah-1 and laccase-1 are each made early, while Luke-2 and Leo-A are each made later, which is consistent with observations of GFP-tagged proteins (Fig. 4D) (33, 35). Western blots of proteins secreted into the culture medium by encysting Ac showed intact laccase-1 and a degraded form of Jonah-1, while Luke-2 and Leo-A were absent. Laccase-1 was detected by a direct ELISA in the culture medium beginning at 12 hours encystation; Jonah-1 appeared later and was less abundant, while Luke-2 and Leo-A were not detected (Fig. 4E).

These results are best explained by a "leaky and sealed" model of cyst wall formation, in which laccase-1 (and Jonah-1) are made early and either bind to cellulose in the partially formed and so leaky outer layer of the wall or are secreted into the medium (Fig. 4F). This is like the large amount of chitinase, which is secreted into the medium by growing *Saccharomyces* (80). In contrast, Luke-2 and Leo-A are made later and either bind to cellulose in the partially formed inner wall or are trapped in the outer wall, which has been completed and is impermeable (35).

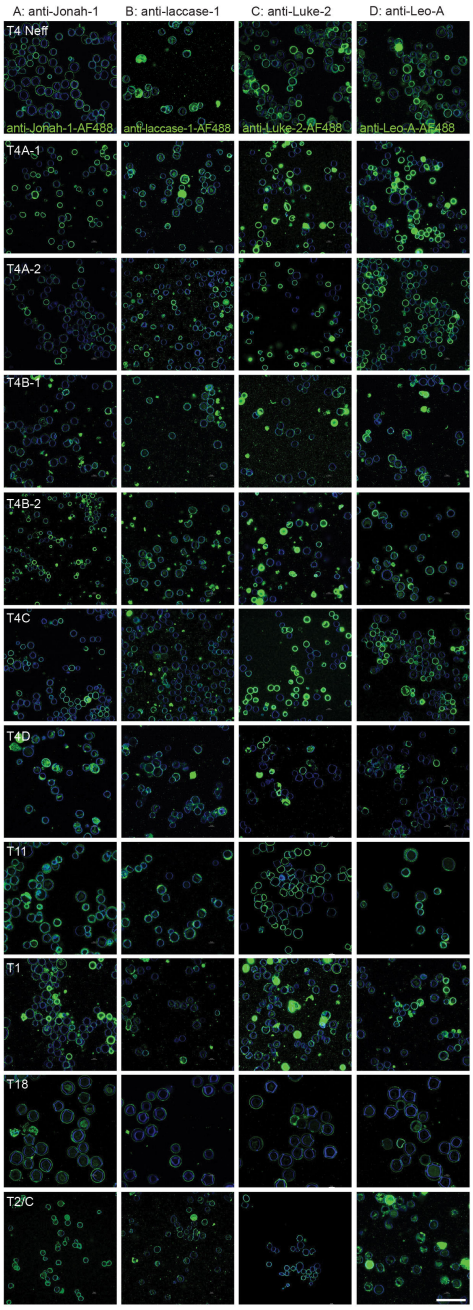

FIG 3 Low-power confocal micrographs show examples of random fields used to determine how efficiently rabbit antibodies to wall proteins detect calcofluor-white-labeled cysts of 10 of the 11 isolates of *Acanthamoeba*. (A–D) Cysts of 11 *Acanthamoeba* isolates (shown at high power in Fig. 2) were labeled with protein A-purified antibodies tagged with Alexa Fluor 488, and the percentage of CFW-tagged cysts detected was counted for two experiments and plotted in Fig. 4A. The purpose of these low-power images is to give an overview of the brightness and homogeneity of the binding of the four rAbs to the 11 *Acanthamoeba* isolates. Note that for counting, individual cysts were visualized at nearly the magnification of cysts in Fig. 2. A single scale bar for panel A–D is 50 µm.

Structural and experimental evidence that an antiparallel β-sandwich (ABS) is the ManBD of the AcMBP-1

While the primary goal here was to identify a simple target for diagnosis of *Acanthamoeba* trophozoites in cultures of corneal scrapings, the secondary goal, which is

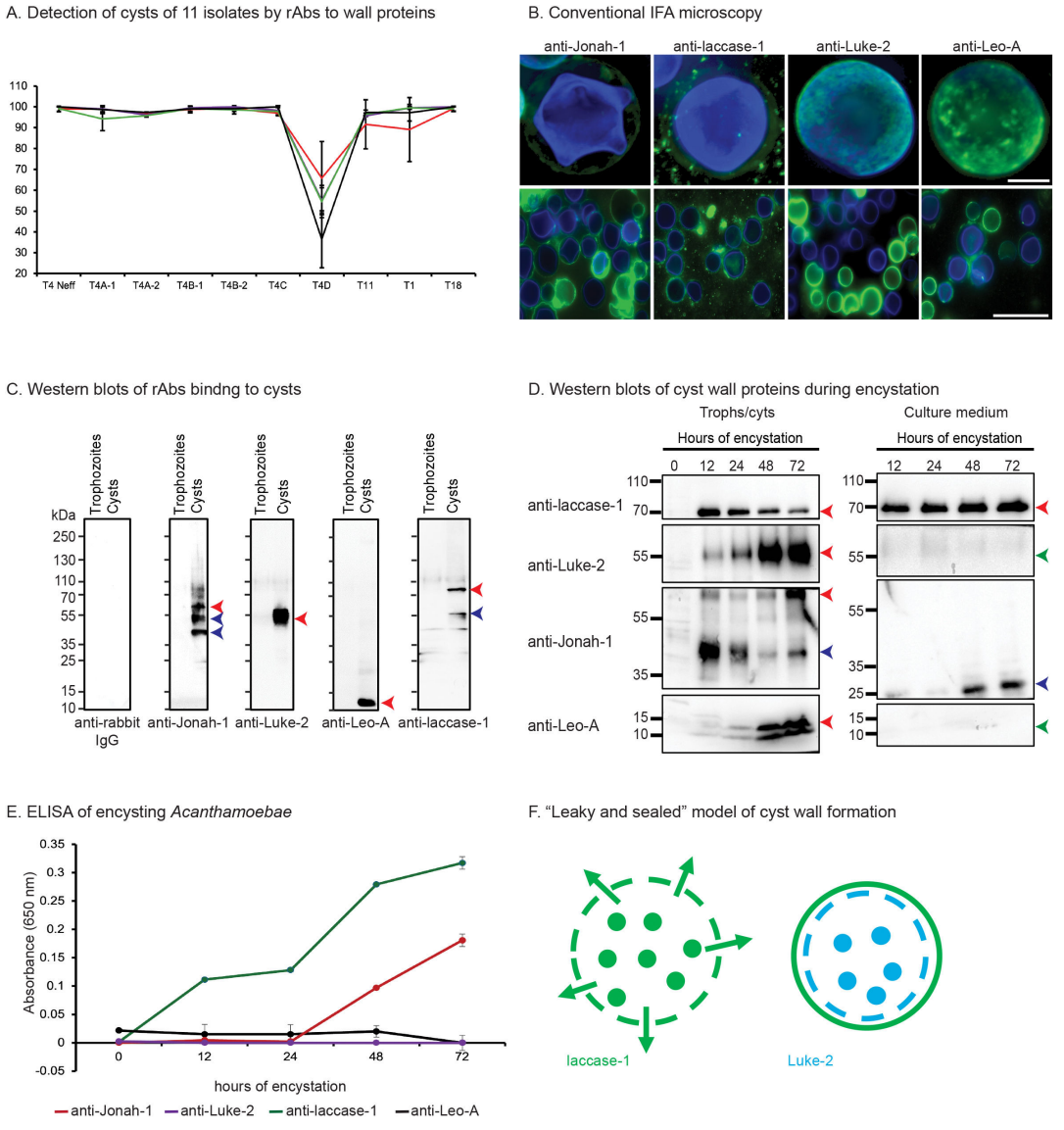

FIG 4 Plots show rAbs to Jonah-1, laccase-1, Luke-2, and Leo-A efficiently detect CFW-labeled cysts, while Western blots and ELISAs identify laccase-1 shed into the medium of encysting Ac. (A) The plot shows the percentage of CFW-labeled cysts detected by four rAbs in three independent experiments (average plus SEM), in which 100+ cysts were counted in random low-power fields (Fig. 3). The rAbs to Luke-2, Leo-A, and laccase-1 each detect >95% of cysts of 10 of the 11 *Acanthamoeba* isolates evaluated, while the rAbs to Jonah-1 are slightly less efficient in detecting 3 isolates of *Acanthamoeba*. The exception is genotype T4C, which is poorly detected with all four rAbs, suggesting a problem with its cyst formation. (B) Rabbit antibodies to four wall proteins also efficiently detect Ac cysts using conventional IFA microscopy. Scale bar for high power is 5 µm and for low power is 50 µm. (C) Western blots show pre-bleeds from rabbits (negative control) fail to bind to proteins of trophozoites or cysts, while rAbs to Jonah-1, Luke-2, Leo-A, and laccase-1 fail to bind to trophozoite proteins (a second negative control) but bind well to cyst proteins of the Neff strain. As discussed in detail in the Results, the anti-Jonah-1 rAbs bind to the expected 55 kDa band (red arrowhead) and two lower mol wt bands (blue arrowheads), while the anti-Luke-2 rAbs bind to a heavy and broad 50 kDa band (red arrowhead), which is greater than the expected size of 27 kDa. The anti-Leo-A rAbs bind to a 13 kDa band (red arrowhead), which is slightly smaller than the expected size of 17 kDA, while the anti-laccase-1 rAbs bind to a 75 kDa band (red arrowhead), which is slightly bigger than the expected size of 64 kDa, as well as to a less abundant 55 kDa band (blue arrowhead). (D) Western blots of whole cell lysates with rAbs (left) show laccase-1 and Jonah-1 are made early in encystation, while Luke-1 and Leo-A are made later in encystation. These results are consistent with the expression of tagged proteins (33). Western blots of culture supernatants (right) show that intact laccase-1 is abundant throughout encystation, while a degraded form of Jonah-1 is abundant at 48- and 72-h encystation. In contrast, neither Luke-2 nor Leo-A are present in the culture medium (green arrowheads). (E) Consistent with Western blots, direct ELISAs of culture supernatants detected laccase-1 throughout encystation; Jonah-1 was detected at 48- and 72-h encystation, while neither Luke-2 nor Leo-A were detected. (F) A "leaky and sealed" model of cyst wall formation suggests some of laccase-1 (and Jonah-1), which is made early, remains bound to the partially completed outer layer of the wall, while the

(Continued on next page)

Fig 4 (Continued)

remaining laccase-1 is secreted into the medium. In contrast, Luke-2 (and Leo-A), which is made later, either binds to the partially completed inner layer of the wall or is trapped in the completed outer layer.

presented first, was to determine the structure and experimentally test the ManBD of AcMBP-1 that mediates adherence to corneal epithelial cells (81). AcMBP-1, which is 833-aa long, was identified in the MEEI 0184 isolate of *Acanthamoeba* (AAT37864 in the NR database at NCBI) but is absent from AmoebaDB (although we identified it in our unpublished transcriptome and proteome of Neff strain of Ac) (8, 9). A recent sequence analysis of AcMBP-1 showed it contains an N-terminal DUF4114 domain, followed by Cys-rich repeats (CRRs), a transmembrane helix, and a ~70 aa cytosolic domain (17). AcMBP-2, which is 360-aa long and is present in AmoebaDB (ACA1_248600), contains the DUF4114 domain but is missing most of the CRRs. Structure predictions of AcMBP-1 showed that the DUF4114 domain is an ABS with four sets of disulfide bonds, which link short loops that are reminiscent of 4DKs of Leo lectins (Fig. 5A and B) (63, 82). The CRRs of AcMBP-1 are composed of numerous pairs of antiparallel β-strands secured at both ends by disulfides (Fig. 5C). Structure searches showed the ABS of AcMBP-1 closely matches that of an uncharacterized protein of *Myxococcus* sp. (30% identity over a 207 amino acid overlap with an *e*-value of 1.4e−13) (Fig. 5D), as well as the ABS of the BclA lectin of *Burkholderia cenocepacia* that has been crystallized with bound methyl α-D-mannoside (12% identity over a 157 amino acid overlap with an *e*-value of 2.3e−2) (Fig. 5E) (66, 83). A maximum-likelihood tree showed that the ABS of AcMBP-1, AcMBP-2, and a third uncharacterized Ac protein (ACA1_173410) derives by horizontal gene transfer (HGT) from bacteria and are absent from other amoebazoa, pathogenic protists, fungi, metazoa, and plants (Fig. 5F) (9, 84–86). Recently, we showed that the BHF of Jonah lectins is also derived by HGT from bacteria (33, 66, 83).

Experimental evidence that the ABS domain is the ManBD of AcMBP-1 included binding of much of an EcMBP-ABS fusion-protein to a mannose-agarose resin, while there was minimal binding of EcMBP alone (blue arrow) (negative control) (Fig. 5G and H). Of note here are (i) the full-length EcMBP-ABS fusion-protein (red arrow) bound best to mannose-agarose resin, while a degradation product (blue arrow) bound very weakly and (ii) EcMBP-ABS failed to elute with excess α-methyl-mannose, suggesting its binding is very tight. In contrast, the mannose-binding plant lectin Concanavalin A (ConA) (red arrow) (positive control) bound well to the mannose-agarose resin and was eluted with α-methyl-mannose, suggesting its binding is less tight (Fig. 5I). EcMBP-ABS and ConA each bound in a similar pattern to the surface and to vesicles associated with microtubules of HCLE cells (Fig. 5J and K). In contrast, EcMBP alone (negative control) failed to bind to HCLE cells (Fig. 5L). In summary, the ABS domain binds mannose and HCLE cells, and so we now refer to it as the ManBD and evaluate it as a diagnostic target for trophozoites (next section).

Finally, to test whether AcMBP might be involved in the cyst wall formation of *Acanthamoeba*, as has been described for the Gal/GalNAc-binding lectin of *Entamoeba* (87), two experiments were performed. First, in contrast to the Gal/GalNAc lectin that binds to glycosylated proteins in the *Entamoeba* cyst wall, EcMBP-ABS fails to bind to proteins in the Ac cyst wall (Fig. 5M). EcMBP-ABS also fails to bind to trophozoites, which explains why *Acanthamoebae* do not self-agglutinate (Fig. 5N). Second, while excess galactose inhibits *Entamoeba* cyst wall formation, even though wall proteins are synthesized and nuclei replicate two times, excess mannose does not inhibit Ac cyst wall formation, visualized with either Jonah-1-mCherry and Luke-2-GFP or laccase-1-RFP and Leo-A-GFP (Fig. 4O).

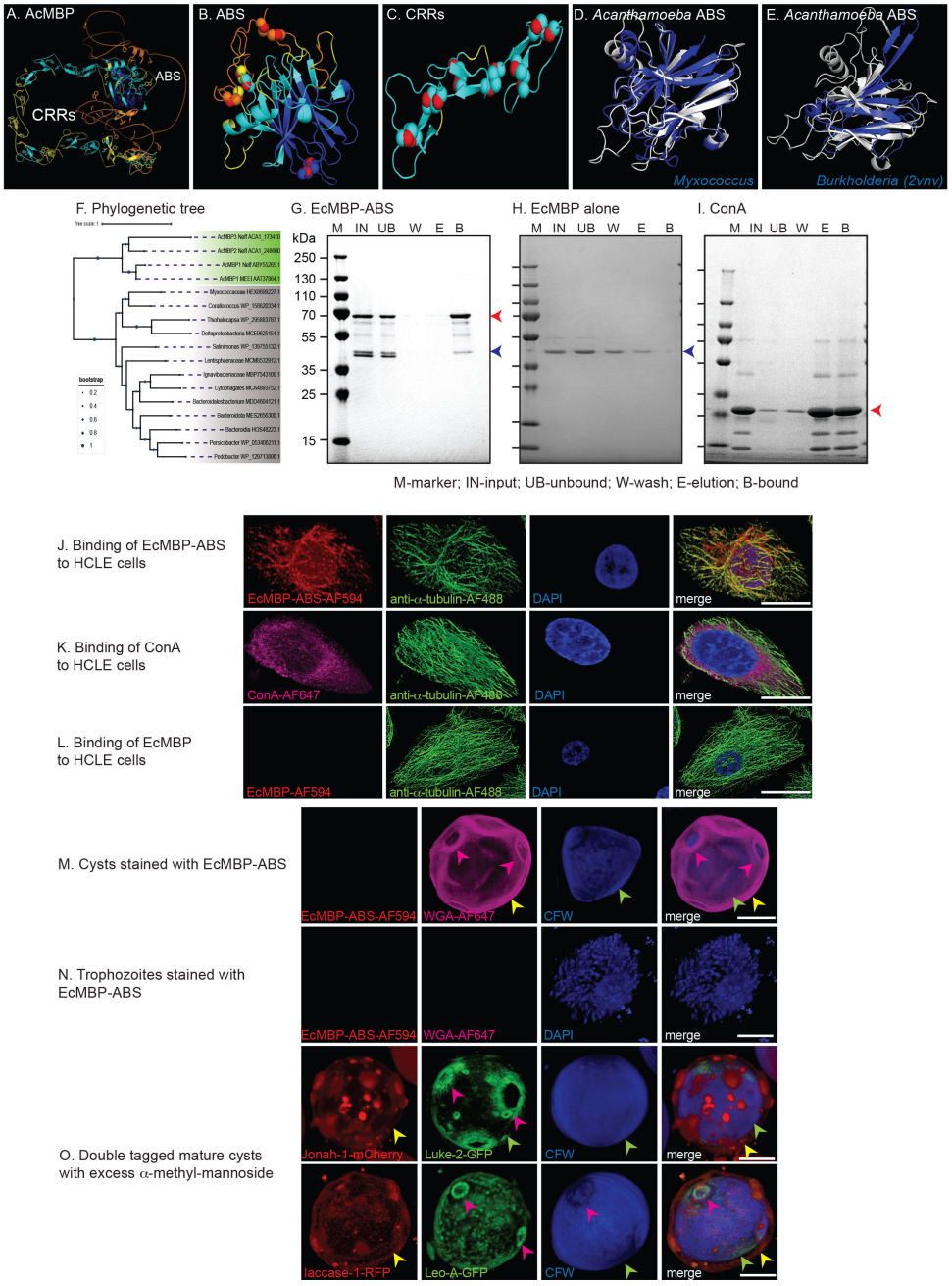

FIG 5 The antiparallel β-sandwich (ABS) of the *Acanthamoeba* mannose-binding protein (AcMBP) binds mannose-agarose resin and human corneal limbal epithelial (HCLE) cells and so is the mannose-binding domain (ManBD). (A) AlphaFold with the confidence-colored shows AcMBP contains an N-terminal ABS and CRRs composed of anti-parallel β-strands. (B and C) The ABS has four loops linked by disulfides, while disulfides also link ends of β-strands in a representative segment of the CRRs. (D and E) Foldseek and PyMOL show that the ABS of AcMBP closely matches the same domain in an uncharacterized protein of *Myxococcus* and is like ManBD of *Burholderia*, which has been crystallized (PDB 2vnv). (F) A maximum-likelihood tree shows ABSs of *Acanthamoeba* MBPs form a cluster, which is distinct from those of bacteria. These results strongly suggest the *Acanthamoeba* ABS derived by HGT, although the precise bacterium cannot be identified. (G) A Western blot shows an *E. coli* maltose-binding protein (EcMBP) fused to ABS binds so strongly to a mannose-agarose resin that it cannot be eluted with excess α-methyl-mannose but can only be released with SDS. (H and I) The negative control EcMBP alone fails to bind to the mannose-agarose resin, while the positive control ConA is eluted from the mannose-agarose resin with excess α-methyl-mannose. (J–L) Confocal microscopy shows EcMBP-ABS and ConA (positive control) each bind to HCLE cells labeled with an anti-tubulin antibody and DAPI, while EcMBP alone (negative control) fails to bind to HCLE cells. (M and N) EcMBP-ABS

(Continued on next page)

Fig 5 (Continued)

does not bind to *Acanthamoeba* cysts or trophozoites. (O) Double labels with Jonah-1-mCherry and Luke-2-GFP or laccase-1 and Leo-A-GFP show incubation with excess α-methyl-mannose has no effect on cyst wall formation. Scale bars for panels J–O are each 5 µm.

Anti-ManBD rAbs efficiently detect trophozoites of all 11 *Acanthamoeba* isolates

BLASTP showed there are many identical amino acid sequences in the ManBDs of AcMBP-1 and AcMBP-2, so that it is likely that the anti-ManBD rAbs will cross-react with both proteins. Similarly, TBLASTN of *Acanthamoeba* genomes in AmoebaDB showed the vast majority have >85% positional identity with ManBD, strongly suggesting that anti-ManBD rAbs will bind well to trophozoites of all *Acanthamoeba* species. Anti-ManBD rAbs, which were made by immunizing a rabbit with the EcMBP-ABS fusion-protein, bound to the surface of trophozoites of the Neff strain (Fig. 6A). DAPI-labeled trophozoites appear blue because *Acanthamoeba* mitochondria have a large genome (~50 kDa each) (88). Pre-bleed rAbs (negative control) failed to bind to trophozoites. Binding of anti-ManBD rAbs to trophozoites was also easily seen using conventional fluorescence microscope (Fig. 6B). High- and low-power confocal micrographs, as well as counts of the latter, showed that anti-ManBD rAbs efficiently detect DAPI-labeled trophozoites of all 11 *Acanthamoeba* isolates tested (Fig. 6C and D).

DISCUSSION

Major conclusions and their limitations

Structural predictions and searches not only helped us identify and characterize cellulose-binding domains of Luke-2 and Leo-A (33) and the ManBD of AcMBP-1 (performed here) but also made it easy to prepare large quantities of recombinant proteins used to immunize rabbits for polyclonal antibodies. Remarkably, abundant wall proteins do not have to be in the ectocyst layer (Jonah-1 and laccase-1) but may be in the endocyst layer (Luke-2 and Leo-A) and still be excellent diagnostic targets for cysts. Further, the binding of rAbs to Jonah-1, Luke-2, Leo-A, and laccase-1 is great enough, so that cysts were easily detected with a conventional fluorescence microscope used in offices of eye doctors or clinical labs. Finally, laccase-1 is shed by encysting *Acanthamoebae*, suggesting the possibility that a lateral flow immunoassay might be used for point-of-care testing (81). Diagnostic anti-cyst rAbs will complement monoclonal antibodies to AcMBP-1 (18, 20–22), as well as antibodies to transporters and secreted proteins (89–91). Anti-cyst antibodies may also supplement PCR assays or Loop-mediated Isothermal Amplification (LAMP) assays for diagnosing AK (92–94). Unfortunately, monoclonal antibodies, PCR, or LAMP assays for diagnosing AK are not presently available even at the best-equipped ophthalmology departments in the United States (44).

The most important limitation here is that the anti-cyst rAbs have not yet been tested by microscopy of corneal scrapings from patients suspected of having AK. These tests demand patient consent forms and approval by the Institutional Review Board and so were not included in these studies, which have only been approved by Institutional Biosafety and Animal Care and Use Committees (see Ethics statement). We have not tested our antibodies versus animal models of AK. The number of *Acanthamoeba* isolates tested was small (11 total), and the genotypes were dominated by T4. There may be strain differences between *Acanthamoebae* of the same genotype, which might cause differences in the properties of their cysts or trophozoites. No attempt was made here to determine the lower limits of parasite density in samples for detection with rAbs by microscopy or by ELISA.

Although we are confident that Luke-2, Leo-A, and Jonah-1 antigens are each unique to Ac, anti-laccase-1 rAbs may cross-react with walls of bacteria, fungi, or plants. Cysts examined here were made by starving cultured *Acanthamoebae* and so might not be the

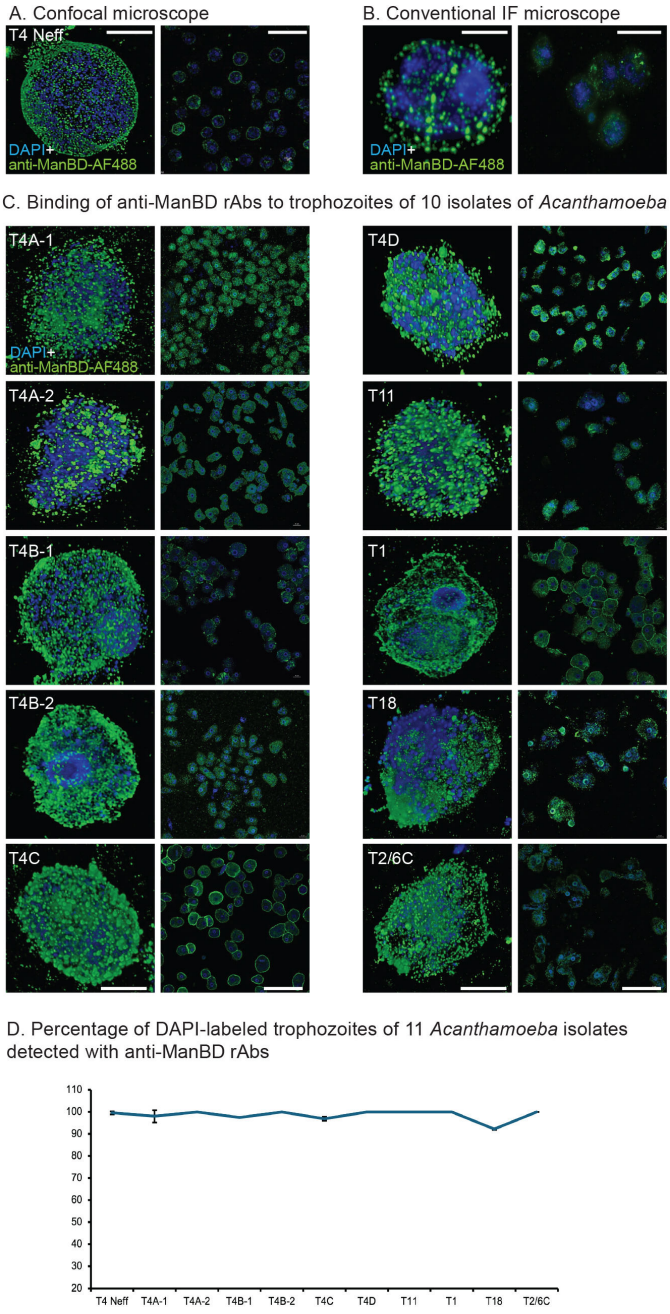

FIG 6 Anti-ManBD rAbs efficiently detect DAPI-labeled trophozoites of all 11 isolates of *Acanthamoeba*. (A) Confocal micrographs show rAbs to EcMBP-ABS, renamed here ManBD, binds to the surface of DAPI-labeled trophozoites of the Neff strain of Ac (high power on left and low power on right). (B) Binding of anti-ManBD rAbs to Neff trophozoites is also easily visualized with conventional immunofluorescent microscope (high power on left and low power on right). (C) Pairs of high power (left) and low power (right) confocal micrographs show anti-ManBD rAbs bind to trophozoites of 10 other isolates *Acanthamoeba*, which were used for binding anti-cyst antibodies in Fig. 2 and 3. (D) Counts of trophozoites in low-power micrographs show that >90% of DAPI-labeled trophozoites were detected by rAbs to the ManBD. (A and B) Scale bars for high-power micrographs are 5 µm and for low-power micrographs are 50 µm.

same as those made in the soil, water, or corneal epithelium. Further, for commercialization, rAbs will have to be replaced by mouse monoclonal antibodies, which are used for

stool diagnosis of walled forms of *Giardia*, *Entamoeba*, and *Cryptosporidium*, or by nanobodies that are used for diagnosis of viruses and bacteria (54–56, 95).

While the DUF4114 had been suggested as the ManBD of AcMBP-1 (17), we used structural predictions, recombinant protein expression, and binding to mannose-agarose resins and HCLE cells to demonstrate that the ABS of AcMBP-1 is indeed the ManBD. Further, we showed that anti-ManBD rAbs to efficiently identify trophozoites from all isolates of *Acanthamoebae* tested. A limitation of our characterization of the ManBD of AcMBP-1 is that we have not performed mutations to identify the amino acids involved in binding mannose on host cell glycoproteins, nor has the ManBD been tested versus arrays of mammalian carbohydrates to determine the precise linkages of terminal mannose to *N*- or *O*-linked glycans (96). Again, rAbs to ManBD need to be tested versus trophozoites cultured from eye scrapings of patients suspected of having AK, while monoclonal antibodies or nanobodies need to be made for the commercialization of anti-ManBD diagnostics.

MATERIALS AND METHODS

Summary of new methods to study candidate targets for diagnosis of *Acanthamoeba* cysts and trophozoites

Methods for culture and encystation of *Acanthamoebae*, protein structure predictions, expression of pairs of tagged cyst wall proteins in transfected parasites, production of EcMBP-fusions in the periplasm of *E. coli*, confocal microscopy, and phylogenetic tree construction were all described in detail in our recent study of the roles of cellulose-binding and timing of expression in targeting of proteins to the cyst wall of the Neff strain of Ac (33). Here, structure predictions were used to identify a candidate ManBD in the AcMBP, which was evaluated by binding of an EcMBP-fusion to a mannose-agarose resin and to HCLE cells. We made rAbs to EcMBP-fusions of four wall proteins and the ManBD and determined their binding to cysts and trophozoites, respectively. An ELISA was used to detect shed wall proteins in the supernatant of encysting Ac. The efficiency of detecting CFW-labeled cysts and DAPI-labeled trophozoites was quantified for 11 *Acanthamoeba* isolates, the identities of which were confirmed by sequencing 18S RNAs. Finally, unless stated otherwise, each experiment was repeated at least three times.

Acanthamoeba genotypes, culture, and cyst preparation

Trophozoites of the Neff strain of Ac (ATCC 30010) were obtained from the American Type Culture Collection (ATCC). Trophozoites of other strains of *Acanthamoeba*, originally derived from human corneal infections and granulomatous encephalitis infections, were received from Dr. Monica Crary, Alcon Research, LLC, Fort Worth, TX, USA, or from Noorjahan Panjwani of Tufts University Medical School (20, 39). Each of these *Acanthamoeba* isolates was confirmed by PCR of 18S RNA, the sequences of which are shown in File S1. Further, a neighbor-joining tree was made to show the similarity of 18S RNA sequences (Fig. S3) (84–86). BLASTN searches for identical 18S RNA sequences were used to determine the genotype of each isolate and to estimate the number and sources of each genotype (8, 9, 11, 12, 14, 67).

Trophozoites were grown and maintained in axenic culture at 30°C in T-75 tissue culture flasks in 10 mL ATCC medium 712 (PYG plus additives) with antibiotics (Pen-Strep) (Sigma-Aldrich Corporation, St. Louis, MO, USA), as described previously (33, 35, 97). Cysts were prepared from trophozoites by incubating them with an encystation medium (EM; 20 mM Tris-HCl [pH 8.8], 100 mM KCl, 8 mM $MgSO_4$, 0.4 mM $CaCl_2$, and 1 mM $NaHCO_3$) for 120 h (98).

Production of EcMBP-fusions containing four cyst wall proteins and the ABS of AcMBP

The production and characterization of EcMBP-fusions containing the BHF of Jonah-1, two BJRFs of Luke-2, two sets of 4DKs of Leo-A, and the CuRO-1 of laccase-1 have all been described (33). The structure of AcMBP was predicted by AlphaFold using the Colab server (63), while the molecular visualization of the ABS of AcMBP, including its four disulfide knots, was performed using PyMOL Molecular Graphics System, Version 2.0 Schrödinger, LLC (99). The ABS structure was then compared with AlphaFold and PDB databases using the Foldseek server (66). Finally, the ABS was made into an EcMBP fusion protein, using the same methods to make EcMBP-fusions containing wall proteins. EcMBP-fusions were made in the pMAL-p2x vector (New England Biolabs) and expressed in BL21-CodonPlus (DE3)-RIPL cells (Agilent Technologies, Lexington, MA, USA) (69, 70). The overexpression of MBP-fusion proteins was induced by the addition of 0.1 mM of IPTG for 16 h at 16°C. MBP-fusion proteins were affinity purified with amylose resin following the manufacturer's instructions (New England Biolabs). The identity and purity of recombinant purified MBP-fusion proteins were confirmed by SDS-PAGE and western immunoblotting analyses.

Generation, IgG purification, and Alexa Fluor-labeling of rAbs

Purified EcMBP-fusions containing four wall proteins and the ABS of AcMBP were used to raise custom rabbit polyclonal antibodies, as per the standard protocol of Cocalico Biologicals, Denver, PA, USA. Total IgG was purified from plasma samples of pre-immune and post-immunized rabbits using affinity chromatography (Pierce Protein A Agarose, Thermo Fisher Scientific, USA). In brief, the serum was first diluted twofold with binding buffer (1× Tris-Buffered Saline, pH 7.4) and loaded onto the top of a column containing Protein A Agarose beads, which were washed with 1× TBS (20-fold column volume). The bound IgG was eluted with 0.1 M glycine-HCl (pH 2.7) into the neutralizing buffer (1 M Tris-HCl, pH 9.0) aliquoted in advance. The elution was concentrated, and the buffer was exchanged against 25 mM Tris-HCl 150 mM NaCl (pH 8.0) using a 30 kDa Amicon Ultra centrifugal filter (Millipore, USA). The purified rAbs were either used as such or further labeled with Alexa Fluor dyes (i.e., 488 and 647) using Invitrogen Fluorescent Protein labeling Kits (Thermo Fisher Scientific), as per the manufacturer's instructions.

Confocal microscopy to compare the localizations of tagged proteins in cyst walls to those of bound rAbs to wall proteins and to determine the efficiency of detecting CFW-tagged cysts with rAbs

The localization of pairs of wall proteins (Jonah-1-mCherrry and Luke-2-GFP or laccase-1-RFP and Leo-A-GFP), each expressed under its own promoter, were previously shown by confocal microscopy of transfected Neff strain cysts (33). Here, the localizations of tagged proteins in intact cysts and walls broken by sonication were compared with localizations of pairs of rAbs (anti-Jonah-1-AF594 and anti-Luke-2-AF488 or anti-laccase-1-AF594 and anti-Leo-A-AF488) binding to intact cysts and broken walls. Intact cysts and broken walls were collected by centrifugation, washed in phosphate-buffered saline (PBS), fixed in 4% paraformaldehyde for 15 min at room temperature, washed again with PBS, and blocked with 1% BSA for 1 h at room temperature. Cysts and walls were then incubated with pairs of tagged rAbs (1:200 dilution) conjugated with AF488 or AF594 for 1 h at room temperature, washed with PBS, and incubated with CFW 1:20 (CFW, 1 mg/mL, Sigma Aldrich) for 30 min at room temperature. The cells were washed three times with 1× PBS and mounted in VECTASHIELD Antifade Mounting Medium (Vector Laboratories, Newark, CA, USA). Cysts were imaged using CFI Plan Apochromat VC 60XC NA 1.42 oil objective of Nikon Ni2 AX inverted confocal microscope equipped with FX-Format F-mount cameras Digital Sight 10 and Digital Sight 50M. We deconvolved 0.1 µm optical sections using NIS elements (Version: AR5.41.02) imaging software. All confocal images shown were 3D reconstructions using dozens of z-stacks. Size bars were based on 2D cross-sections.

To determine how well rAbs to four wall proteins detect cysts of 11 isolates of *Acanthamoeba*, we collected mature cysts (120 h in encystation medium) from each isolate, which were washed in PBS, fixed in 4% washed again, and blocked with BSA, as described above. The cysts were incubated with unlabeled rAbs to each wall protein, which was detected as secondary anti-rabbit IgG conjugated with Alexa Fluor 488 (1:300) and CFW. Confocal images were captured with the 60× objective and 3D reconstructions were performed to determine whether rAbs bound to the ectocyst layer, endocyst layer, and/or ostioles. In addition, at least 100 cysts in random fields were counted to determine what percentage of CFW-labeled cysts of each isolate were detected with each rAb. Each experiment was repeated three times, and the counts for the two experiments were averaged. Finally, we examined the same set of slides with a Plan-APO Chromat 100× oil immersion lens on a Zeiss Axio Observer Z1 microscope equipped with Axio Cam ERc5s to determine whether a confocal microscope is needed to detect the binding of rAbs to trophozoites or cysts.

Western blotting and ELISA of wall proteins in trophozoites, cysts, and medium of encysting *Acanthamoebae*

To detect the cyst wall proteins in the Neff strain of Ac, we harvested log-phase trophozoites and mature cysts (120 h in encystation medium) and lysed them in an SDS sample buffer. The lysates were separated on SDS-PAGE gel (4–15%), transferred to a nitrocellulose membrane, and blocked with 5% BSA in PBS. The blots were probed with rAbs (1:5,000) or purified rabbit IgG (1:1,000) raised against the different abundant cyst wall proteins. Anti-rabbit IgG conjugated to HRP (Thermo Fisher Scientific) was used as the secondary antibody. Rabbit pre-immune serum or anti-rabbit IgG was used as a control. Super Signal West Pico PLUS (Thermo Fisher Scientific) substrate was used for chemiluminescent detection. Blots were imaged using GE ImageQuant LAS 4000 gel imager.

To detect cyst wall proteins in encysting Ac and their culture supernatant, we encysted trophozoites of the Neff strain, and the cell pellet and culture supernatant were collected at 0, 12, 24, 48, and 72 h. To remove the possibility of intact cells, we precleared the supernatant by three rounds of centrifugation at 3,000 × *g* for 10 min at 4°C. The supernatant was subjected to an additional centrifugation step (10,000 × *g*, 10 min at 4°C) and concentrated using a 3 kDa Amicon Ultra centrifugal filter (Millipore, USA). The protein concentration in each sample was determined by DC protein assay (Bio-Rad, Hercules CA, 500-011). The presence of candidate cyst wall proteins in concentrated culture supernatant was studied by western blotting and direct ELISA methods (33). For western blotting analysis, a total of 50 µg protein from each time point were separated on SDS-PAGE gel (4–20%), transferred to nitrocellulose membrane, and probes, as described above. For direct ELISA, the flat bottom microtiter plates (Nunc-Immuno MicroWell 96-well solid plates) were coated overnight with 50 µL of the culture supernatants diluted to a final concentration of 50 µg/mL in carbonate buffer. Negative controls were carbonate buffer alone or trophozoite culture medium. The microtiter plates were blocked with 200 µL blocking buffer (3% BSA/PBS) at room temperature for 2 h and washed three times with PBS/Tween-20. The plate was subsequently incubated with either control pre-immune rabbit IgG or immunized rabbit purified IgG diluted 1:3,000 for 2 h, washed, and incubated with anti-rabbit HRP conjugated secondary antibody diluted 1:6,000. Plates were washed and then developed using TMB ELISA substrate (Abcam, Ab171522), and the absorbance was recorded at 370 nm. The OD of each sample dilution was calculated as the OD of the protein-coated wells minus the OD of the buffer-coated wells.

Characterization of the ManBD (also known as ABS) of AcMBP and binding of anti-ManBD rAbs to trophozoites

To determine whether the ABS of AcMBP is the ManBD, we made an EcMBP-ABS fusion protein in the periplasm of *E. coli,* and we evaluated its ability to bind to

mannose-agarose resin (Sigma) and HCLE cells. EcMBP-ABS was allowed to bind to mannose-agarose resin for 1 h at 4°C in the binding buffer (0.1 M Tris buffer, pH 7.2, 100 mM NaCl, and 20 mM $CaCl_2$). The beads were washed three times, and the bound fraction was initially eluted using excess mannose (0.1 M α-Man) and then by boiling the beads in 2× SDS-PAGE sample buffer. EcMBP alone was a negative control, while ConA (Vector Laboratories) was a positive control. The samples were further analyzed by electrophoresis in 4–20% SDS-polyacrylamide gel.

HCLE cells, which were a gift from Vickery Trinkaus-Randall of Boston University Medical Center, were grown in keratinocyte serum-free medium (KSFM) with the following supplements: 25 µg/mL bovine pituitary extract, 0.02 nM EGF, 0.3 mM $CaCl_2$, 100 U/mL penicillin, and 100 µg/mL streptomycin (100). HCLE cells were grown to confluence in 3 mm glass bottom culture discs, fixed with 4% paraformaldehyde at room temperature for 15 min, washed three times with 1× PBS, and blocked with 1% BSA for 1 h at room temperature. HCLE cells were stained with 10 µg of the EcMBP-ABS fusion-protein conjugated with AF594 along with anti-alpha tubulin antibody (Sigma) conjugated with AF488 for 1 h at room temperature. HCLE cells were also incubated with EcMBP alone conjugated with AF594 (negative control) or ConA conjugated with AF647 (positive control. Subsequently, the HCLE cells were washed three times with 1× PBS, mounted in VECTASHIELD Antifade Mounting Medium (Vector Laboratories, Newark, CA, USA), and visualized using 488 nm (Alexa Fluor 488) and 594 nm (Alexa Fluor 594) laser excitation.

rAbs to EcMBP-ABS, which are referred to as anti-ManBD rAbs, were made, purified, and labeled with AF488, as described above for rAbs to cyst wall proteins. Dividing trophozoites from 11 isolates of *Acanthamoeba*, which were used to test the binding to CFW-labeled cysts by rAbs to wall proteins, were collected by centrifugation, washed three times with PBS, and fixed in 4% paraformaldehyde for 15 min at room temperature. The cells were labeled with anti-ManBD rAbs, labeled with DAPI, and visualized with high-power confocal microscopy, as described above. In three separate experiments, low-power images of 100+ trophozoites were captured and counted to determine the efficiency of detection of DAPI-labeled trophozoites of each isolate. Finally, anti-ManBD rAbs bound to trophozoites of the Neff strain of Ac were visualized with a conventional Zeiss Axio Observer Z1 microscope.

ACKNOWLEDGMENTS

Thanks go to Dr. Monica Crary of Alcon Research and Dr. Noorjahan Panjwani of Tufts University Medical School for isolates of *Acanthamoeba* studied here. Thanks to go Dr. Thomas Dohlman of the Massachusetts Eye and Ear for informing us as to the availability (or lack thereof) of diagnostic tests for AK.

This work was supported in part by grants to J.S. from National Institutes of Health (R01 GM129324) and from Howard Hughes Medical Institute (Emerging Pathogens Initiative).

B.K.S. and M.G. each designed, performed, and analyzed the experiments, as well as prepared figures and wrote a draft of the paper. J.S. provided funding, supervised the work, and finished authoring the paper.

AUTHOR AFFILIATION

[1]Department of Molecular and Cell Biology, Boston University Goldman School of Dental Medicine, Boston, Massachusetts, USA

AUTHOR ORCIDs

Bharath Kanakapura Sundararaj http://orcid.org/0000-0002-2891-3106
Manish Goyal http://orcid.org/0000-0003-2383-5409
John Samuelson http://orcid.org/0000-0001-9533-3040

FUNDING

Funder	Grant(s)	Author(s)
HHS | National Institutes of Health (NIH)	R01 GM129324	John Samuelson
Howard Hughes Medical Institute (HHMI)	Emerging Pathogens Initiative (EPI)	John Samuelson

AUTHOR CONTRIBUTIONS

Bharath Kanakapura Sundararaj, Conceptualization, Data curation, Formal analysis, Investigation, Methodology, Validation, Writing – original draft | Manish Goyal, Conceptualization, Data curation, Formal analysis, Investigation, Methodology, Validation, Writing – original draft | John Samuelson, Conceptualization, Funding acquisition, Investigation, Methodology, Supervision, Writing – original draft, Writing – review and editing

ETHICS APPROVAL

Culture and manipulation of *Acanthamoebae* under BSL-2 protocols were approved by the Boston University Institutional Biosafety Committee. Production of custom rabbit antibodies was approved by the Institutional Animal Care and Use Committee of Cocalico Biologics, Inc., Denver, PA, USA.

ADDITIONAL FILES

The following material is available online.

Supplemental Material

File S1 (mSphere00948-24-s0001.xlsx). Sequences, genotypes, and sources of 11 *Acanthamoeba* isolates studied here.
Supplemental figures (mSphere00948-24-s0002.docx). Fig. S1 to S3.

REFERENCES

1. Abd El Wahab WM, El-Badry AA, Hamdy DA. 2018. Molecular characterization and phylogenetic analysis of *Acanthamoeba* isolates in tap water of Beni-Suef, Egypt. Acta Parasitol 63:826–834. https://doi.org/10.1515/ap-2018-0101
2. Lorenzo-Morales J, Khan NA, Walochnik J. 2015. An update on *Acanthamoeba* keratitis: diagnosis, pathogenesis and treatment. Parasite 22:10. https://doi.org/10.1051/parasite/2015010
3. Zbiba W, Abdesslem NB. 2018. *Acanthamoeba* keratitis: an emerging disease among microbial keratitis in the Cap Bon region of Tunisia. Exp Parasitol 192:42–45. https://doi.org/10.1016/j.exppara.2018.05.005
4. Zhong J, Li X, Deng Y, Chen L, Zhou S, Huang W, Lin S, Yuan J. 2017. Associated factors, diagnosis and management of *Acanthamoeba* keratitis in a referral Center in Southern China. BMC Ophthalmol 17:175. https://doi.org/10.1186/s12886-017-0571-7
5. Brown AC, Ross J, Jones DB, Collier SA, Ayers TL, Hoekstra RM, Backensen B, Roy SL, Beach MJ, Yoder JS, Acanthamoeba Keratitis Investigation T. 2018. Risk factors for *Acanthamoeba* keratitis-a multistate case-control study, 2008-2011. Eye Contact Lens 44 Suppl 1:S173–S178. https://doi.org/10.1097/ICL.0000000000000365
6. Carnt Nicole, Hoffman JJ MBBS, Verma S, Hau S, Radford CF, Minassian DC, Dart JKG. 2018. *Acanthamoeba* keratitis: confirmation of the UK outbreak and a prospective case-control study identifying contributing risk factors. Br J Ophthalmol 102:1621–1628. https://doi.org/10.1136/bjophthalmol-2018-312544
7. Carnt N, Stapleton F. 2016. Strategies for the prevention of contact lens-related *Acanthamoeba* keratitis: a review. Ophthalmic Physiol Opt 36:77–92. https://doi.org/10.1111/opo.12271
8. Amos B, Aurrecoechea C, Barba M, Barreto A, Basenko EY, Bażant W, Belnap R, Blevins AS, Böhme U, Brestelli J, et al. 2022. VEuPathDB: the eukaryotic pathogen, vector and host bioinformatics resource center. Nucleic Acids Res 50:D898–D911. https://doi.org/10.1093/nar/gkab929
9. Clarke M, Lohan AJ, Liu B, Lagkouvardos I, Roy S, Zafar N, Bertelli C, Schilde C, Kianianmomeni A, Bürglin TR, et al. 2013. Genome of *Acanthamoeba castellanii* highlights extensive lateral gene transfer and early evolution of tyrosine kinase signaling. Genome Biol 14:R11. https://doi.org/10.1186/gb-2013-14-2-r11
10. Coronado-Velázquez D, Silva-Olivares A, Castro-Muñozledo F, Lares-Jiménez LF, Rodríguez-Anaya LZ, Shibayama M, Serrano-Luna J. 2020. *Acanthamoeba* mauritaniensis genotype T4D: an environmental isolate displays pathogenic behavior. Parasitol Int 74:102002. https://doi.org/10.1016/j.parint.2019.102002
11. Diehl MLN, Paes J, Rott MB. 2021. Genotype distribution of *Acanthamoeba* in keratitis: a systematic review. Parasitol Res 120:3051–3063. https://doi.org/10.1007/s00436-021-07261-1
12. Fuerst PA. 2023. The status of molecular analyses of isolates of *Acanthamoeba* maintained by international culture collections. Microorganisms 11:295. https://doi.org/10.3390/microorganisms11020295
13. Fuerst PA, Booton GC. 2020. Species, sequence types and alleles: dissecting genetic variation in *Acanthamoeba*. Pathogens 9:534. https://doi.org/10.3390/pathogens9070534
14. Fuerst PA, Booton GC, Crary M. 2015. Phylogenetic analysis and the evolution of the 18S rRNA gene typing system of *Acanthamoeba*. J Eukaryot Microbiol 62:69–84. https://doi.org/10.1111/jeu.12186
15. Yera H, Zamfir O, Bourcier T, Viscogliosi E, Noël C, Dupouy-Camet J, Chaumeil C. 2008. The genotypic characterisation of *Acanthamoeba* isolates from human ocular samples. Br J Ophthalmol 92:1139–1141. https://doi.org/10.1136/bjo.2007.132266
16. Wang Y, Jiang L, Zhao Y, Ju X, Wang L, Jin L, Fine RD, Li M. 2023. Biological characteristics and pathogenicity of *Acanthamoeba*. Front Microbiol 14:1147077. https://doi.org/10.3389/fmicb.2023.1147077
17. Corsaro D. 2022. *Acanthamoeba* mannose and laminin binding proteins variation across species and genotypes. Microorganisms 10:2162. https://doi.org/10.3390/microorganisms10112162
18. Garate M, Alizadeh H, Neelam S, Niederkorn JY, Panjwani N. 2006. Oral immunization with *Acanthamoeba castellanii* mannose-binding protein

ameliorates amoebic keratitis. Infect Immun 74:7032–7034. https://doi.org/10.1128/IAI.00828-06
19. Garate M, Cao Z, Bateman E, Panjwani N. 2004. Cloning and characterization of a novel mannose-binding protein of *Acanthamoeba*. J Biol Chem 279:29849–29856. https://doi.org/10.1074/jbc.M402334200
20. Garate M, Cubillos I, Marchant J, Panjwani N. 2005. Biochemical characterization and functional studies of *Acanthamoeba* mannose-binding protein. Infect Immun 73:5775–5781. https://doi.org/10.1128/IAI.73.9.5775-5781.2005
21. Garate M, Marchant J, Cubillos I, Cao Z, Khan NA, Panjwani N. 2006. *In vitro* pathogenicity of *Acanthamoeba* is associated with the expression of the mannose-binding protein. Invest Ophthalmol Vis Sci 47:1056–1062. https://doi.org/10.1167/iovs.05-0477
22. Kang AY, Park AY, Shin HJ, Khan NA, Maciver SK, Jung SY. 2018. Production of a monoclonal antibody against a mannose-binding protein of *Acanthamoeba culbertsoni* and its localization. Exp Parasitol 192:19–24. https://doi.org/10.1016/j.exppara.2018.07.009
23. Büchele MLC, Nunes BF, Filippin-Monteiro FB, Caumo KS. 2023. Diagnosis and treatment of *Acanthamoeba* keratitis: a scoping review demonstrating unfavorable outcomes. Cont Lens Anterior Eye 46:101844. https://doi.org/10.1016/j.clae.2023.101844
24. Carrijo-Carvalho LC, Sant'ana VP, Foronda AS, de Freitas D, de Souza Carvalho FR. 2017. Therapeutic agents and biocides for ocular infections by free-living amoebae of *Acanthamoeba* genus. Surv Ophthalmol 62:203–218. https://doi.org/10.1016/j.survophthal.2016.10.009
25. Di Zazzo A, De Gregorio C, Coassin M. 2024. Novel effective medical therapy for *Acanthamoeba* keratitis. Eye Contact Lens 50:279–281. https://doi.org/10.1097/ICL.0000000000001092
26. Kaufman AR, Tu EY. 2022. Advances in the management of *Acanthamoeba* keratitis: a review of the literature and synthesized algorithmic approach. Ocul Surf 25:26–36. https://doi.org/10.1016/j.jtos.2022.04.003
27. Loufouma-Mbouaka A, Martín-Pérez T, Köhsler M, Danisman Z, Schwarz M, Mazumdar R, Samba-Louaka A, Walochnik J. 2024. Characterization of novel extracellular proteases produced by *Acanthamoeba castellanii* after contact with human corneal epithelial cells and their relevance to pathogenesis. Parasit Vectors 17:242. https://doi.org/10.1186/s13071-024-06304-7
28. Marcelino I, Samba-Louaka A, Rice CA. 2024. Editorial: new advances in the biology and pathogenesis of free-living amoebae. Front Microbiol 15:1401217. https://doi.org/10.3389/fmicb.2024.1401217
29. Michalek M, Sönnichsen FD, Wechselberger R, Dingley AJ, Hung C-W, Kopp A, Wienk H, Simanski M, Herbst R, Lorenzen I, Marciano-Cabral F, Gelhaus C, Gutsmann T, Tholey A, Grötzinger J, Leippe M. 2013. Structure and function of a unique pore-forming protein from a pathogenic *Acanthamoeba*. Nat Chem Biol 9:37–42. https://doi.org/10.1038/nchembio.1116
30. Shing B, Balen M, McKerrow JH, Debnath A. 2021. *Acanthamoeba* keratitis: an update on amebicidal and cysticidal drug screening methodologies and potential treatment with azole drugs. Expert Rev Anti Infect Ther 19:1427–1441. https://doi.org/10.1080/14787210.2021.1924673
31. Bernard C, Locard-Paulet M, Noël C, Duchateau M, Giai Gianetto Q, Moumen B, Rattei T, Hechard Y, Jensen LJ, Matondo M, Samba-Louaka A. 2022. A time-resolved multi-omics atlas of *Acanthamoeba castellanii* encystment. Nat Commun 13:4104. https://doi.org/10.1038/s41467-022-31832-0
32. Bowers B, Korn ED. 1969. The fine structure of *Acanthamoeba castellanii* (Neff strain). II. Encystment. J Cell Biol 41:786–805. https://doi.org/10.1083/jcb.41.3.786
33. Kanakapura Sundararaj B, Goyal M, Samuelson J. 2024. Cellulose binding and the timing of expression influence protein targeting to the double-layered cyst wall of *Acanthamoeba* mSphere 9:e00466-24. https://doi.org/10.1128/msphere.00466-24
34. Lloyd D. 2014. Encystment in *Acanthamoeba castellanii*: a review. Exp Parasitol 145 Suppl:S20–S27. https://doi.org/10.1016/j.exppara.2014.03.026
35. Magistrado-Coxen P, Aqeel Y, Lopez A, Haserick JR, Urbanowicz BR, Costello CE, Samuelson J. 2019. The most abundant cyst wall proteins of *Acanthamoeba castellanii* are lectins that bind cellulose and localize to distinct structures in developing and mature cyst walls. PLoS Negl Trop Dis 13:e0007352. https://doi.org/10.1371/journal.pntd.0007352
36. Benton WF, Wilborn M. 1964. Induction of synchronous encystment (differentiation) in *Acanthamoeba* spp. Methods Cell Biol 1:55–83. https://doi.org/10.1016/S0091-679X(08)62086-5
37. Potter JL, Weisman RA. 1976. Cellulose synthesis by extracts of *Acanthamoeba castellanii* during encystment. Stimulation of the incorporation of radioactivity from UDP-(14C)glucose into alkali-soluble and insoluble beta-glucans by glucose 6-phosphate and related compounds. Biochim Biophys Acta 428:240–252. https://doi.org/10.1016/0304-4165(76)90125-2
38. Aqeel Y, Rodriguez R, Chatterjee A, Ingalls RR, Samuelson J. 2017. Killing of diverse eye pathogens (*Acanthamoeba* spp., *Fusarium solani*, and *Chlamydia trachomatis*) with alcohols. PLoS Negl Trop Dis 11:e0005382. https://doi.org/10.1371/journal.pntd.0005382
39. Campolo A, Pifer R, Walters R, Thomas M, Miller E, Harris V, King J, Rice CA, Shannon P, Patterson B, Crary M. 2022. *Acanthamoeba* spp. aggregate and encyst on contact lens material increasing resistance to disinfection. Front Microbiol 13:1089092. https://doi.org/10.3389/fmicb.2022.1089092
40. Coulon C, Collignon A, McDonnell G, Thomas V. 2010. Resistance of *Acanthamoeba* cysts to disinfection treatments used in health care settings. J Clin Microbiol 48:2689–2697. https://doi.org/10.1128/JCM.00309-10
41. Dupuy M, Berne F, Herbelin P, Binet M, Berthelot N, Rodier M-H, Soreau S, Héchard Y. 2014. Sensitivity of free-living amoeba trophozoites and cysts to water disinfectants. Int J Hyg Environ Health 217:335–339. https://doi.org/10.1016/j.ijheh.2013.07.007
42. Pittet D, Allegranzi B, Boyce J, World Health Organization World Alliance for Patient Safety First Global Patient Safety Challenge Core Group of Experts. 2009. The world health organization guidelines on hand hygiene in health care and their consensus recommendations. Infect Control Hosp Epidemiol 30:611–622. https://doi.org/10.1086/600379
43. Walters R, Campolo A, Miller E, McAnally C, Gabriel M, Shannon P, Crary M. 2022. Differential antimicrobial efficacy of preservative-free contact lens disinfection systems against common ocular pathogens. Microbiol Spectr 10:e02138-21. https://doi.org/10.1128/spectrum.02138-21
44. Azzopardi M, Chong YJ, Ng B, Recchioni A, Logeswaran A, Ting DSJ. 2023. Diagnosis of *Acanthamoeba* keratitis: past, present and future. Diagnostics (Basel) 13:2655. https://doi.org/10.3390/diagnostics13162655
45. Bouten M, Elsheikha HM. 2022. Diagnosis and management of *Acanthamoeba* keratitis: a continental approach. Parasitologia 2:167–197. https://doi.org/10.3390/parasitologia2030016
46. Chidambaram JD, Prajna NV, Palepu S, Lanjewar S, Shah M, Elakkiya S, Macleod D, Lalitha P, Burton MJ. 2018. *In vivo* confocal microscopy cellular features of host and organism in bacterial, fungal, and *Acanthamoeba keratitis*. Am J Ophthalmol 190:24–33. https://doi.org/10.1016/j.ajo.2018.03.010
47. Li S, Bian J, Wang Y, Wang S, Wang X, Shi W. 2020. Clinical features and serial changes of *Acanthamoeba* keratitis: an *in vivo* confocal microscopy study. Eye (Lond) 34:327–334. https://doi.org/10.1038/s41433-019-0482-3
48. Varacalli G, Di Zazzo A, Mori T, Dohlman TH, Spelta S, Coassin M, Bonini S. 2021. Challenges in *Acanthamoeba* keratitis: a review. J Clin Med 10:942. https://doi.org/10.3390/jcm10050942
49. Zhang Y, Xu X, Wei Z, Cao K, Zhang Z, Liang Q. 2023. The global epidemiology and clinical diagnosis of *Acanthamoeba* keratitis. J Infect Public Health 16:841–852. https://doi.org/10.1016/j.jiph.2023.03.020
50. Orlean P. 2012. Architecture and biosynthesis of the *Saccharomyces cerevisiae* cell wall. Genetics 192:775–818. https://doi.org/10.1534/genetics.112.144485
51. West CM. 2003. Comparative analysis of spore coat formation, structure, and function in *Dictyostelium*. Int Rev Cytol 222:237–293. https://doi.org/10.1016/s0074-7696(02)22016-1
52. Wilhelmus KR, Osato MS, Font RL, Robinson NM, Jones DB. 1986. Rapid diagnosis of *Acanthamoeba* keratitis using calcofluor white. Arch Ophthalmol 104:1309–1312. https://doi.org/10.1001/archopht.1986.01050210063026
53. Zablackis E, Huang J, Müller B, Darvill AG, Albersheim P. 1995. Characterization of the cell-wall polysaccharides of *Arabidopsis thaliana* leaves. Plant Physiol 107:1129–1138. https://doi.org/10.1104/pp.107.4.1129

54. Arrowood MJ, Sterling CR. 1989. Comparison of conventional staining methods and monoclonal antibody-based methods for *Cryptosporidium oocyst* detection. J Clin Microbiol 27:1490–1495. https://doi.org/10.1128/jcm.27.7.1490-1495.1989
55. Spadafora LJ, Kearney MR, Siddique A, Ali IK, Gilchrist CA, Arju T, Hoffstrom B, Nguyen FK, Petri WA, Haque R, Cangelosi GA. 2016. Species-specific immunodetection of an *Entamoeba histolytica* cyst wall protein. PLoS Negl Trop Dis 10:e0004697. https://doi.org/10.1371/journal.pntd.0004697
56. Stibbs HH. 1989. Monoclonal antibody-based enzyme immunoassay for *Giardia lamblia* antigen in human stool. J Clin Microbiol 27:2582–2588. https://doi.org/10.1128/jcm.27.11.2582-2588.1989
57. Bateman E. 2010. Expression plasmids and production of EGFP in stably transfected *Acanthamoeba*. Protein Expr Purif 70:95–100. https://doi.org/10.1016/j.pep.2009.10.008
58. Peng Z, Omaruddin R, Bateman E. 2005. Stable transfection of *Acanthamoeba castellanii*. Biochim Biophys Acta 1743:93–100. https://doi.org/10.1016/j.bbamcr.2004.08.014
59. Enguita FJ, Martins LO, Henriques AO, Carrondo MA. 2003. Crystal structure of a bacterial endospore coat component. A laccase with enhanced thermostability properties. J Biol Chem 278:19416–19425. https://doi.org/10.1074/jbc.M301251200
60. Hanada Y, Nishimiya Y, Miura A, Tsuda S, Kondo H. 2014. Hyperactive antifreeze protein from an Antarctic sea ice bacterium *Colwellia* sp. has a compound ice-binding site without repetitive sequences. FEBS J 281:3576–3590. https://doi.org/10.1111/febs.12878
61. Liu Z, Xie T, Zhong Q, Wang G. 2016. Crystal structure of CotA laccase complexed with 2,2-azinobis-(3-ethylbenzothiazoline-6-sulfonate) at a novel binding site. Acta Crystallogr F Struct Biol Commun 72:328–335. https://doi.org/10.1107/S2053230X1600426X
62. Boraston AB, Bolam DN, Gilbert HJ, Davies GJ. 2004. Carbohydrate-binding modules: fine-tuning polysaccharide recognition. Biochem J 382:769–781. https://doi.org/10.1042/BJ20040892
63. Jumper J, Evans R, Pritzel A, Green T, Figurnov M, Ronneberger O, Tunyasuvunakool K, Bates R, Žídek A, Potapenko A, et al. 2021. Highly accurate protein structure prediction with AlphaFold. Nature New Biol 596:583–589. https://doi.org/10.1038/s41586-021-03819-2
64. Lombard V, Golaconda Ramulu H, Drula E, Coutinho PM, Henrissat B. 2014. The carbohydrate-active enzymes database (CAZy) in 2013. Nucleic Acids Res 42:D490–5. https://doi.org/10.1093/nar/gkt1178
65. Urbanowicz BR, Catalá C, Irwin D, Wilson DB, Ripoll DR, Rose JKC. 2007. A tomato endo-beta-1,4-glucanase, SlCel9C1, represents a distinct subclass with a new family of carbohydrate binding modules (CBM49). J Biol Chem 282:12066–12074. https://doi.org/10.1074/jbc.M607925200
66. van Kempen M, Kim SS, Tumescheit C, Mirdita M, Lee J, Gilchrist CLM, Söding J, Steinegger M. 2024. Fast and accurate protein structure search with Foldseek. Nat Biotechnol 42:243–246. https://doi.org/10.1038/s41587-023-01773-0
67. Rayamajhee B, Sharma S, Willcox M, Henriquez FL, Rajagopal RN, Shrestha GS, Subedi D, Bagga B, Carnt N. 2022. Assessment of genotypes, endosymbionts and clinical characteristics of *Acanthamoeba* recovered from ocular infection. BMC Infect Dis 22:757. https://doi.org/10.1186/s12879-022-07741-4
68. Gipson IK, Spurr-Michaud S, Argüeso P, Tisdale A, Ng TF, Russo CL. 2003. Mucin gene expression in immortalized human corneal-limbal and conjunctival epithelial cell lines. Invest Ophthalmol Vis Sci 44:2496–2506. https://doi.org/10.1167/iovs.02-0851
69. Duong-Ly KC, Gabelli SB. 2015. Affinity purification of a recombinant protein expressed as a fusion with the maltose-binding protein (MBP) tag. Methods Enzymol 559:17–26. https://doi.org/10.1016/bs.mie.2014.11.004
70. Kapust RB, Waugh DS. 1999. *Escherichia coli* maltose-binding protein is uncommonly effective at promoting the solubility of polypeptides to which it is fused. Protein Sci 8:1668–1674. https://doi.org/10.1110/ps.8.8.1668
71. Altschul SF, Madden TL, Schäffer AA, Zhang J, Zhang Z, Miller W, Lipman DJ. 1997. Gapped BLAST and PSI-BLAST: a new generation of protein database search programs. Nucleic Acids Res 25:3389–3402. https://doi.org/10.1093/nar/25.17.3389
72. Finn RD, Attwood TK, Babbitt PC, Bateman A, Bork P, Bridge AJ, Chang H-Y, Dosztányi Z, El-Gebali S, Fraser M, et al. 2017. InterPro in 2017-beyond protein family and domain annotations. Nucleic Acids Res 45:D190–D199. https://doi.org/10.1093/nar/gkw1107
73. Matthey-Doret C, Colp MJ, Escoll P, Thierry A, Moreau P, Curtis B, Sahr T, Sarrasin M, Gray MW, Lang BF, Archibald JM, Buchrieser C, Koszul R. 2022. Chromosome-scale assemblies of *Acanthamoeba castellanii* genomes provide insights into *Legionella pneumophila* infection-related chromatin reorganization. Genome Res 32:1698–1710. https://doi.org/10.1101/gr.276375.121
74. Janusz G, Pawlik A, Świderska-Burek U, Polak J, Sulej J, Jarosz-Wilkołazka A, Paszczyński A. 2020. Laccase properties, physiological functions, and evolution. Int J Mol Sci 21:966. https://doi.org/10.3390/ijms21030966
75. Satlin MJ, Graham JK, Visvesvara GS, Mena H, Marks KM, Saal SD, Soave R. 2013. Fulminant and fatal encephalitis caused by *Acanthamoeba* in a kidney transplant recipient: case report and literature review. Transpl Infect Dis 15:619–626. https://doi.org/10.1111/tid.12131
76. Hayrapetyan H, Tran T, Tellez-Corrales E, Madiraju C. 2023. Enzyme-linked immunosorbent assay: types and applications. Methods Mol Biol 2612:1–17. https://doi.org/10.1007/978-1-0716-2903-1_1
77. Gupta R, Brunak S. 2002. Prediction of glycosylation across the human proteome and the correlation to protein function. Pac Symp Biocomput:310–322.
78. Schiller B, Makrypidi G, Razzazi-Fazeli E, Paschinger K, Walochnik J, Wilson IBH. 2012. Exploring the unique N-glycome of the opportunistic human pathogen *Acanthamoeba*. J Biol Chem 287:43191–43204. https://doi.org/10.1074/jbc.M112.418095
79. Steentoft C, Vakhrushev SY, Joshi HJ, Kong Y, Vester-Christensen MB, Schjoldager KT-BG, Lavrsen K, Dabelsteen S, Pedersen NB, Marcos-Silva L, Gupta R, Bennett EP, Mandel U, Brunak S, Wandall HH, Levery SB, Clausen H. 2013. Precision mapping of the human O-GalNAc glycoproteome through SimpleCell technology. EMBO J 32:1478–1488. https://doi.org/10.1038/emboj.2013.79
80. Kuranda MJ, Robbins PW. 1991. Chitinase is required for cell separation during growth of *Saccharomyces cerevisiae*. J Biol Chem 266:19758–19767.
81. Li G, Li Q, Wang X, Liu X, Zhang Y, Li R, Guo J, Zhang G. 2023. Lateral flow immunoassays for antigens, antibodies and haptens detection. Int J Biol Macromol 242:125186. https://doi.org/10.1016/j.ijbiomac.2023.125186
82. Varadi M, Anyango S, Deshpande M, Nair S, Natassia C, Yordanova G, Yuan D, Stroe O, Wood G, Laydon A, et al. 2022. AlphaFold Protein Structure Database: massively expanding the structural coverage of protein-sequence space with high-accuracy models. Nucleic Acids Res 50:D439–D444. https://doi.org/10.1093/nar/gkab1061
83. Lameignere E, Malinovská L, Sláviková M, Duchaud E, Mitchell EP, Varrot A, Sedo O, Imberty A, Wimmerová M. 2008. Structural basis for mannose recognition by a lectin from opportunistic bacteria *Burkholderia cenocepacia*. Biochem J 411:307–318. https://doi.org/10.1042/bj20071276
84. Edgar RC. 2004. MUSCLE: multiple sequence alignment with high accuracy and high throughput. Nucleic Acids Res 32:1792–1797. https://doi.org/10.1093/nar/gkh340
85. Kumar S, Stecher G, Li M, Knyaz C, Tamura K. 2018. MEGA X: molecular evolutionary genetics analysis across computing platforms. Mol Biol Evol 35:1547–1549. https://doi.org/10.1093/molbev/msy096
86. Letunic I, Bork P. 2021. Interactive Tree Of Life (iTOL) v5: an online tool for phylogenetic tree display and annotation. Nucleic Acids Res 49:W293–W296. https://doi.org/10.1093/nar/gkab301
87. Frisardi M, Ghosh SK, Field J, Van Dellen K, Rogers R, Robbins P, Samuelson J. 2000. The most abundant glycoprotein of amebic cyst walls (Jacob) is a lectin with five Cys-rich, chitin-binding domains. Infect Immun 68:4217–4224. https://doi.org/10.1128/IAI.68.7.4217-4224.2000
88. Gawryluk RMR, Chisholm KA, Pinto DM, Gray MW. 2014. Compositional complexity of the mitochondrial proteome of a unicellular eukaryote (*Acanthamoeba castellanii*, supergroup Amoebozoa) rivals that of animals, fungi, and plants. J Proteomics 109:400–416. https://doi.org/10.1016/j.jprot.2014.07.005
89. Kim DY, Son DH, Matin A, Jung SY. 2021. Production of a monoclonal antibody against a galactose-binding protein of *Acanthamoeba castellanii* and its cytotoxicity. Parasitol Res 120:3845–3850. https://doi.org/10.1007/s00436-021-07321-6
90. Kim MJ, Chu KB, Lee HA, Quan FS, Kong HH, Moon EK. 2022. Detection of *Acanthamoeba* spp. using carboxylesterase antibody and its usage for diagnosing *Acanthamoeba*-keratitis. PLoS One 17:e0262223. https://doi.org/10.1371/journal.pone.0262223
91. Weber-Lima MM, Prado-Costa B, Becker-Finco A, Costa AO, Billilad P, Furst C, de Moura JF, Alvarenga LM. 2020. *Acanthamoeba* spp.

monoclonal antibody against a CPA2 transporter: a promising molecular tool for acanthamoebiasis diagnosis and encystment study. Parasitology 147:1678–1688. https://doi.org/10.1017/S0031182020001778
92. Aykur M, Karakavuk M, Akıl M, Can H, Döşkaya M, Gürüz AY, Dağcı H, Değirmenci Döşkaya A. 2023. Development and sensitivity determination of *18S rRNA* gene-specific fast loop-mediated isothermal amplification (LAMP) assay for rapid detection of *Acanthamoeba* Turkiye Parazitol Derg 47:129–135. https://doi.org/10.4274/tpd.galenos.2023.46362
93. Mewara A, Khurana S, Yoonus S, Megha K, Tanwar P, Gupta A, Sehgal R. 2017. Evaluation of loop-mediated isothermal amplification assay for rapid diagnosis of *Acanthamoeba* keratitis. Indian J Med Microbiol 35:90–94. https://doi.org/10.4103/ijmm.IJMM_16_227
94. Reddy AK, Balne PK, Reddy RK, Mathai A, Kaur I. 2011. Loop-mediated isothermal amplification assay for the diagnosis of retinitis caused by herpes simplex virus-1. Clin Microbiol Infect 17:210–213. https://doi.org/10.1111/j.1469-0691.2010.03216.x
95. Naidoo DB, Chuturgoon AA. 2023. The potential of nanobodies for COVID-19 diagnostics and therapeutics. Mol Diagn Ther 27:193–226. https://doi.org/10.1007/s40291-022-00634-x
96. Heimburg-Molinaro J, Mehta AY, Tilton CA, Cummings RD. 2024. Insights into glycobiology and the protein-glycan interactome using glycan microarray technologies. Mol Cell Proteomics. https://doi.org/10.1016/j.mcpro.2024.100844:100844
97. Jensen T, Barnes WG, Meyers D. 1970. Axenic cultivation of large populations of *Acanthamoeba castellanii* (JBM). J Parasitol 56:904–906.
98. Neff RJ, Ray SA, Benton WF, Wilborn M. 1964. Induction of synchronous encystment (differentiation) in *Acanthamoeba* spp. Methods Cell Biol 1:55–83. https://doi.org/10.1016/S0091-679X(08)62086-5
99. Rigsby RE, Parker AB. 2016. Using the PyMOL application to reinforce visual understanding of protein structure. Biochem Mol Biol Educ 44:433–437. https://doi.org/10.1002/bmb.20966
100. Onochie OE, Onyejose AJ, Rich CB, Trinkaus-Randall V. 2020. The role of hypoxia in corneal extracellular matrix deposition and cell motility. Anat Rec (Hoboken) 303:1703–1716. https://doi.org/10.1002/ar.24110